



Cite this: DOI: 10.1039/d0dt00689k

Peptoid-based siderophore mimics as dinuclear Fe<sup>3+</sup> chelators†Assunta D'Amato, ‡<sup>a</sup> Pritam Ghosh, ‡<sup>b</sup> Chiara Costabile, <sup>a</sup>  
Giorgio Della Sala, <sup>a</sup> Irene Izzo, <sup>a</sup> Galia Maayan \*<sup>b</sup> and  
Francesco De Riccardis \*<sup>a</sup>

A practical synthesis of preorganized tripodal enterobactin/corynebactin-type ligands (consisting of a C<sub>3</sub>-symmetric macrocyclic peptoid core, three catecholamide coordinating units, and C<sub>2</sub>, C<sub>4</sub>, and C<sub>6</sub> spacers) is reported. The formation of complexes with Fe<sup>3+</sup> was investigated by spectrophotometric (UV-Vis) and spectrometric (ESI, negative ionization mode) methods and corroborated by theoretical (DFT) calculations. Preliminary studies revealed the intricate interplay between the conformational chirality of cyclic trimeric peptoids and metal coordination geometry of mononuclear species similar to that of natural catechol-based siderophores. Experimental results demonstrated the unexpected formation of unique dinuclear Fe<sup>3+</sup> complexes.

Received 24th February 2020,  
Accepted 4th April 2020

DOI: 10.1039/d0dt00689k

rsc.li/dalton

## Introduction

Naturally occurring and synthetic siderophores are of great interest not only due to their vital role in microorganisms, plants and fungi,<sup>1,2</sup> but also due to their growing clinical relevance as antibiotic carriers<sup>3</sup> and inhibitors of metalloenzymes,<sup>3</sup> in imaging<sup>4</sup> and in the treatment of iron overload disease.<sup>5</sup>

Due to its redox active nature, excess of iron in human body, caused by transfusion due to anaemic disorders, induces organ malfunction and failure. Iron chelation therapy (ICT) restores the physiological concentrations of this metal making use of high-affinity iron-chelating compounds. Unfortunately, most of the commercially available ferric iron sequestering agents (*i.e.*: deferoxamine, deferiprone, and deferasirox) show multiple adverse side effects (neutropenia, neurotoxicity, agranulocytosis, diarrhoea, and hepatic/cardiac damage)<sup>6,7</sup> and search for new families of iron chelators is an ebullient field of research.<sup>1-4</sup>

Natural products have always been the most successful source of inspiration for the design of new drugs and entero-

bactin/corynebactin<sup>8</sup> bacterial siderophores enclose quintessential attributes for the synthesis of artificial iron chelators. The presence of three convergent catecholamide (1,2-dihydroxybenzamide) units, stemming from a twelve-membered macrocyclic core, promotes chiroselective trapping of ferric ions in natural siderophores (Fig. 1). In particular, [Fe(enterobactin)]<sup>3-</sup>, [Fe(1)]<sup>3-</sup>, displays a right-handed ( $\Delta$ ) coordination mode<sup>9</sup> and [Fe(corynebactin)]<sup>3-</sup>, [Fe(2)]<sup>3-</sup>, shows a left-handed ( $\Lambda$ ) chirality of the Fe<sup>3+</sup> centre.<sup>9</sup>

Although **1** and **2** are powerful iron chelators,<sup>1</sup> the hydrolytic instability of ester linkages<sup>10</sup> present in the macrocyclic core, encouraged the synthesis of novel, more stable, and biocompatible siderophores.<sup>4,11</sup>

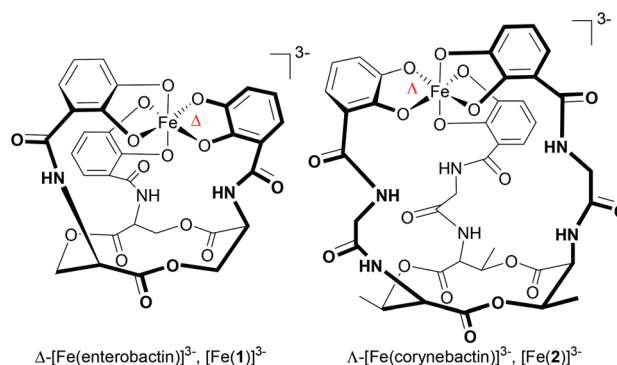


Fig. 1 Molecular structure and absolute configuration for the Fe<sup>3+</sup> tris chelate centre ( $\Delta$  or  $\Lambda$ ) of naturally occurring enterobactin (**1**) and corynebactin (**2**) metal complexes.

<sup>a</sup>Department of Chemistry and Biology "A. Zambelli", University of Salerno, Via Giovanni Paolo II, 132, Fisciano, SA, 84084, Italy. E-mail: dericca@unisa.it

<sup>b</sup>Schulich Faculty of Chemistry, Technion – Israel Institute of Technology, Haifa, 32000, Israel. E-mail: gm92@technion.ac.il

† Electronic supplementary information (ESI) available: NMR spectra, HPLC chromatograms of linear and cyclic peptoids, UV titration with metal ions, ESI-MS of Fe<sup>3+</sup> complexes, and computational details. See DOI: 10.1039/D0DT00689K

‡ Equal contribution.

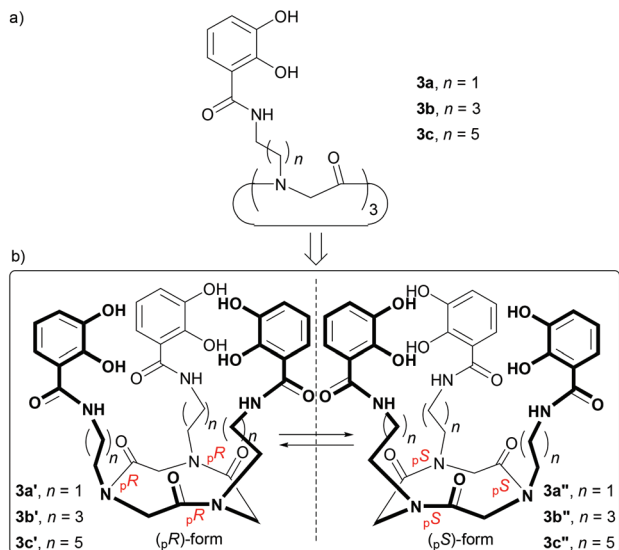


**Fig. 2** (a) Molecular structures of cyclotrimeric peptoid catecholamides **3a-c**. (b) Possible enantiomeric forms of cyclopeptoid-based hosts showing opposite conformational chirality ( $(pR)$ -form: **3a'-c'** and  $(pS)$ -form: **3a''-c''**).

With the aim to find a novel robust cyclooligomeric frame for catecholamide chelating groups, we designed a new family of siderophores based on a proteolytically/hydrolytically stable<sup>12</sup> peptoid scaffold displaying  $C_2$ ,  $C_4$ , and  $C_6$  spacers and a preorganized cyclotrimeric structure (**3a-c**, Fig. 2a).

The presence of a sterically strained nine-membered macrocycle<sup>13</sup> and a relatively high thermodynamic barrier for the oligoamide ring interconversion ( $\Delta G^\ddagger \approx 19$  kcal mol<sup>-1</sup>, for cyclic tripeptoids)<sup>13,14</sup> indicated the formation of **3a'-c'/3a''-c''** enantiomeric conformational isomers, with opposite planar chirality at the tertiary amide bond centres (Fig. 2b).<sup>13,15</sup>

In the present contribution we report the synthesis of cyclooligomeric **3a-c**, as amide-based analogues of enterobactin/corynebactin-type siderophores. In this study we reveal their conformational properties as free hosts and Fe<sup>3+</sup> complexes, and demonstrate, through accurate spectrophotometric/spectrometric analyses, the formation of unique dinuclear complexes.

## Results and discussion

### DFT studies on mononuclear complexes

The concurrent presence of amide bonds at stereogenic sites<sup>13,15</sup> and left- $(\Lambda)$  or right-handed ( $\Delta$ ) coordination geometry<sup>9</sup> at the Fe<sup>3+</sup> centre, leads to the formation of energetically nonequivalent metal-cyclopeptoid complexes with  $p_R/\Lambda$ ;  $p_R/\Delta$  and  $p_S/\Delta$ ;  $p_S/\Lambda$  configurations.

To obtain the lowest energy conformation and a quantum mechanical refinement, density functional theory (DFT) calculations at the B3LYP/6-311G\* level were performed on the model with the  $C_2$  spacer and  $p_R$  amide bond configuration

(**3a'**). Theoretically calculated structures of the diastereomeric  $\Lambda$ -[Fe(**3a'**)]<sup>3-</sup> and  $\Delta$ -[Fe(**3a'**)]<sup>3-</sup> models (Fig. 3a) indicated an internal energy difference ( $\Delta E$ ) equal to 3.3 kcal mol<sup>-1</sup> in favor of the former species (Fig. 3b), suggesting a steric mismatch between the  $p_R$  planar chirality and  $\Delta$  configuration of the metal centre.

The higher stability of the  $p_R/\Lambda$  diastereoisomer was attributed to a modest dihedral angle distortion of complex  $\Lambda$ -[Fe(**3a'**)]<sup>3-</sup> ( $\Delta\phi \approx +7^\circ$ ;  $\Delta\psi \approx +4^\circ$ ;  $\Delta\omega \approx -9^\circ$ ) when compared to the classic CP<sub>1</sub>  $\gamma$ -turn values reported for cyclic trimeric peptoids ( $\phi = +95^\circ$ ;  $\psi = -95^\circ$ ;  $\omega = 0^\circ$ ).<sup>16</sup> The average deviations estimated for the higher energy species  $\Delta$ -[Fe(**3a'**)]<sup>3-</sup> were more pronounced ( $\Delta\phi \approx +17^\circ$ ;  $\Delta\psi \approx +17^\circ$ ,  $\Delta\omega \approx -27.0^\circ$ , see the ESI† for atomic coordinates).

Ring size shrinkage from twelve-membered natural oligolactones **1** and **2** to nine-membered cyclopeptoid hosts **3a-c** was considered uninfluential for the iron complex formation with tricatechol-based ligands, as MECAM and TRENCAM, with smaller 1,3,5-trisaminomethylbenzene<sup>11d</sup> and  $\beta$ ,  $\beta'$ ,  $\beta''$ -triaminotriethylamine<sup>11c,e</sup> cores, display excellent iron-chelating activity.

The main problem to be addressed, in the experimental studies, was heterogeneous nuclearity typical of the catecholamide complexes.<sup>11b,f</sup>

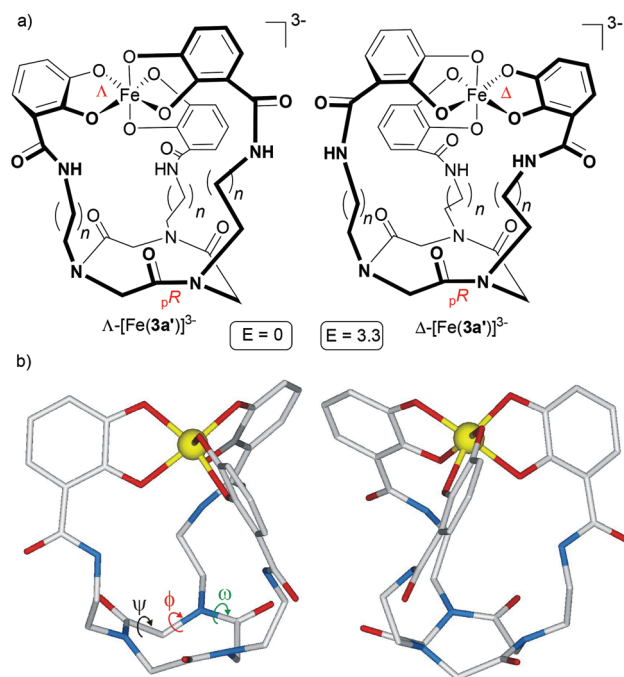
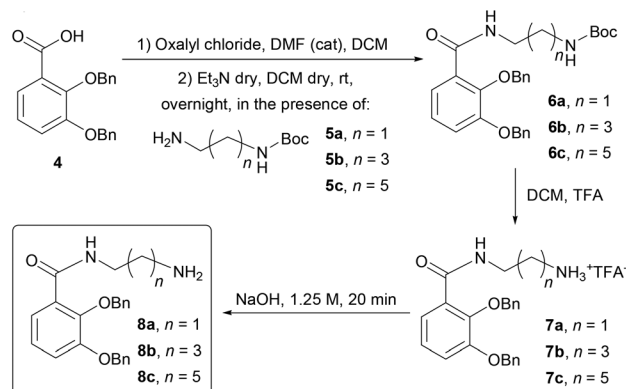


**Fig. 3** (a) Schematic structures of cyclopeptoid complexes  $\Lambda$ -[Fe-**3a'**]<sup>3-</sup> and  $\Delta$ -[Fe-**3a'**]<sup>3-</sup>. (b) Minimum energy structures of  $\Lambda$ -[Fe-**3a'**]<sup>3-</sup> and  $\Delta$ -[Fe-**3a'**]<sup>3-</sup> and their respective internal energies calculated at the B3LYP/6-311G\* level of theory expressed in kcal mol<sup>-1</sup> (see the ESI† for Cartesian coordinates). Dihedral angle definition for residue  $i$ :  $\omega$  [ $C\alpha_{(i-1)}$ ;  $CO_{(i-1)}$ ;  $N_{(i)}$ ;  $C\alpha_{(i)}$ ],  $\phi$  [ $CO_{(i-1)}$ ;  $N_{(i)}$ ;  $C\alpha_{(i)}$ ;  $CO_{(i)}$ ],  $\psi$  [ $N_{(i)}$ ;  $C\alpha_{(i)}$ ;  $CO_{(i)}$ ;  $N_{(i+1)}$ ]. Hydrogen atoms are omitted for clarity. Atom type: C light grey, N blue, O red, and Fe yellow.



**Scheme 1** Synthesis of *N*-( $\omega$ -aminoalkyl)-2,3-bis(benzyloxy)benzamide intermediates **8a–c**.

### Synthesis of cyclic peptoid ligands **3a–c**

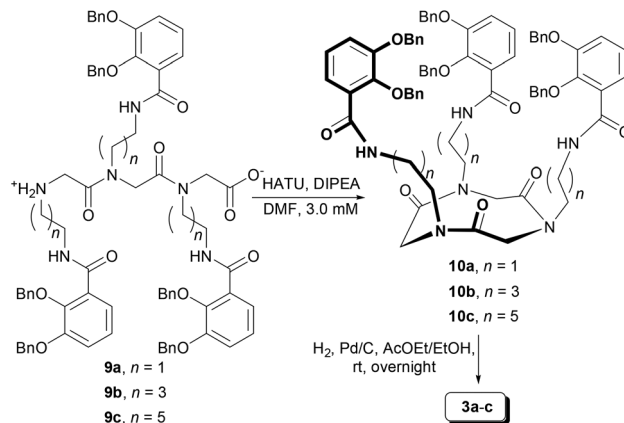
The synthesis of enterobactin/corynebactin peptoid analogues **3a–c** relied on the solid-phase “sub-monomer” approach<sup>17</sup> and required preliminary elaboration of the appropriately protected primary amines for their insertion in the growing oligoamide chain. The amine precursors were known *N*-(2-aminoethyl)-2,3-bis(benzyloxy)benzamide<sup>18</sup> (**8a**) and *N*-(4-aminobutyl)-2,3-bis(benzyloxy)benzamide<sup>19</sup> (**8b**), plus new *N*-(6-aminoethyl)-2,3-bis(benzyloxy)benzamide (**8c**) intermediates. **8a–c** were synthesized according the general procedure<sup>18</sup> reported in Scheme 1.

The formation of 2,3-bis(benzyloxy)benzoyl chloride<sup>20</sup> from the corresponding acid **4** and subsequent amidation in the presence of mono-Boc diamines **5a–c**,<sup>21</sup> gave the required fully protected amidocarbamates **6a–c**. The acid-induced *N*-Boc deprotection and formation of the corresponding free bases produced the primary amines **8a–c** useful for solid-phase synthesis.

Intermediates **8a–c** readily reacted with the bromoacetic residues of the growing peptoid chains, according to the classic solid phase procedure<sup>17</sup> and gave linear oligoamides **9a–c** (Scheme 2) in an excellent overall yield with decent analytical purity (see the ESI†).

Linear peptoids **9a–c** were successfully cyclized in the presence of an efficient HATU condensing agent under high dilution conditions (3.0 mM). The fully protected targets **10a–c** were subsequently isolated as all-*cis* “crown” conformational isomers.<sup>13,22</sup> *C*<sub>3</sub>-symmetry, in accordance with previously synthesized cyclic trimeric peptoid congeners,<sup>23,24</sup> was inferred by the revelation of one third of the expected <sup>1</sup>H and <sup>13</sup>C NMR signals of **10a–c** (<sup>1</sup>H NMR analysis, 600 MHz, CDCl<sub>3</sub>, see the ESI†). The presence of *cis* amide bonds was supported by the extensive X-ray/NMR/modelling studies on similar cyclic tripeptoids.<sup>13,22</sup>

Variable temperature <sup>1</sup>H NMR experiments on strained *N,N',N''*-tri-2,3-bis(benzyloxy)benzamidethyl-*cyclo*-triglycine **10a** demonstrated, for the diastereotopic glycine protons, no coalescence up to 373 K (C<sub>2</sub>D<sub>2</sub>Cl<sub>4</sub> solution, 600 MHz, implying  $\Delta G^\ddagger > 16.9$  kcal mol<sup>-1</sup>), confirming the presence, at room



**Scheme 2** Final steps of the synthetic route of tris-catecholamide ligands **3a–c**. For simplicity, enantiomorphous conformational isomers were not reported.

temperature, of conformational isomers in slow equilibrium on the NMR time scale.<sup>25</sup>

Catalytic debenzoylation in the presence of H<sub>2</sub> and Pd/C afforded the cyclic catecholamides **3a–c** in quantitative yields. All-*cis* “crown” conformations of the target 2,3-dihydroxycatecholamides were established on the basis of the three-fold symmetry present in the <sup>1</sup>H and <sup>13</sup>C NMR spectra (600 MHz, CD<sub>3</sub>OD, see the ESI†). The inequivalence of intra-annular glycine proton resonances ( $\Delta\delta \sim 1.5$  ppm) inferred the presence of conformational enantiomers **3a'–c'**/**3a''–c''** in slow equilibrium on the NMR time scale.

### Metal ion binding studies

Metal-free peptoids **3a–c** exhibited three absorption bands each, in methanol, arising from 2,3-dihydroxybenzamide.<sup>26</sup> Upon addition of FeCl<sub>3</sub>, the intensity of these three bands increased and new absorption bands were obtained, indicating that all three peptoids bind with Fe<sup>3+</sup>. For **3a**, the bands near  $\lambda = 209, 251$  and  $316$  nm, shifted upon binding with Fe<sup>3+</sup> to  $\lambda_{\text{max}} = 215, 258$  and  $322$  nm, respectively (Fig. 4a). Similarly, for **3b** the bands near  $\lambda = 207, 250$  and  $318$  nm were shifted to  $211$  nm with a shoulder at  $227$  nm,  $258$  nm and  $330$  with a shoulder at  $365$  nm, respectively (Fig. 4b). For **3c**, a similar trend was observed and the bands near  $\lambda = 208, 248$  and  $314$  nm shifted to  $209$  nm with a shoulder at  $227$  nm,  $258$  and  $332$  nm with a shoulder at  $363$  nm, respectively (Fig. 4c). In addition to these shifts, a new band near  $\lambda = 570, 562$  and  $565$  nm for **3a–c**, respectively, was obtained, due to ligand-to-metal charge transfer (LMCT), indicating the formation of bis (catecholate) rather than tris(catecholate) complexes.<sup>27,28</sup> From these UV-Vis titration results, metal-to-peptoid ratio plots were constructed, revealing a saturation of the absorbance value at a 2 : 1 ratio for the Fe<sup>3+</sup> : peptoid.

The Job's plot,<sup>29</sup> obtained by monitoring the absorbance at  $570$  nm with  $17 \mu\text{M}$  Fe<sup>3+</sup> and varying the concentrations of **3a** in methanol (Fig. S14a, ESI†) also indicated a 2 : 1 Fe<sup>3+</sup> : **3a** ratio, supporting the coordination of two Fe<sup>3+</sup> ions to each

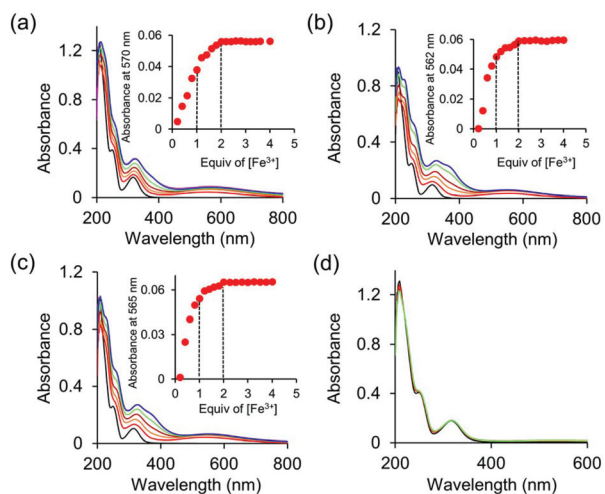
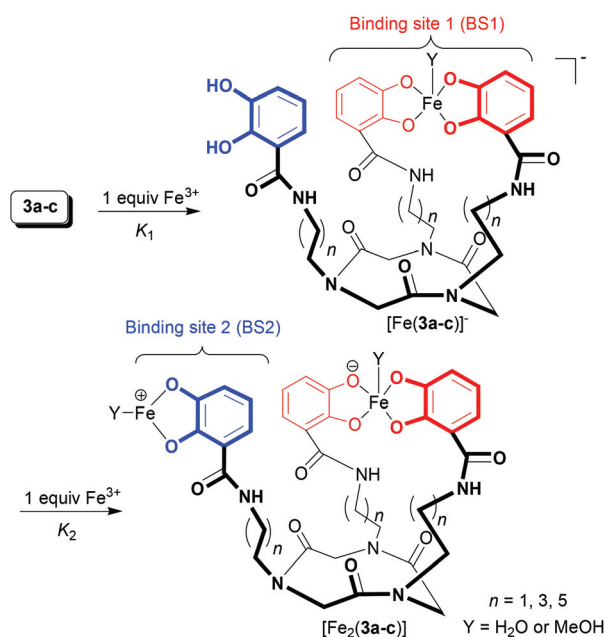


**Fig. 4** UV-Vis titration of: (a–c) **3a–c** (17 μM in methanol) with additions of 2 μL aliquots of 5 mM methanol solution of Fe<sup>3+</sup> in multiple steps (black: free peptoid and blue: Fe<sup>3+</sup> complex) (d) **3a** (17 μM in methanol) with additions of 2 μL aliquots of 5 mM methanol solution of Fe<sup>2+</sup> in multiple steps (black: free peptoid and green: peptoid without interaction with the Fe<sup>2+</sup> ion).

peptoid rather than 1 : 1 binding. Interestingly, a rapid linear increase in the intensity of each LMCT band was observed until one equiv. of the Fe<sup>3+</sup> ions was added (Fig. 4a–c, insets). Further addition of another equiv. of Fe<sup>3+</sup> ions led to a slower gradual intensity increase, reaching the saturation upon two equiv. addition (Fig. 4a–c, insets).

Rationalization of the experimental results has been recapitulated in Scheme 3. The first equivalent of Fe<sup>3+</sup> is captured by



**Scheme 3** Proposed two-step coordination of peptoids **3a–c** to two equiv. of Fe<sup>3+</sup> with the formation of zwitterionic species [Fe<sub>2</sub>(**3a–c**)].

two catechol ligands (binding site 1, BS1, in red colour), forming bis(catecholate)Fe<sup>3+</sup> complexes, [Fe(**3a–c**)]<sup>–</sup>, with a certain number of solvent molecules (methanol and/or water) depending on the Fe<sup>3+</sup> coordination geometry. The second equiv. of the Fe<sup>3+</sup> ions binds to the remaining catechol ligand (binding site 2, BS2, in blue colour) to give the hypothesized dinuclear complex [Fe<sub>2</sub>(**3a–c**)] (plus methanol and/or water molecules).

We also suggest that the mononuclear complex [Fe(**3a–c**)]<sup>–</sup> is formed upon the first addition of one equiv. of the Fe<sup>3+</sup> ions, such that  $K_1 \gg K_2$ , assuming a stronger (and faster) binding to the two catechol chelators of BS1.<sup>30</sup>

Interestingly, the titration of **3a–c** with Fe<sup>2+</sup> did not produce any observable changes in the UV-Vis spectra, indicating that these peptoids do not bind with Fe<sup>2+</sup>. The UV-Vis titration of **3a** with Fe<sup>2+</sup> is depicted in Fig. 4d (see the ESI† for **3b–c**). The UV-Vis titration of peptoids **3a–c** with Co<sup>2+</sup>, Cu<sup>2+</sup>, Ni<sup>2+</sup> and Zn<sup>2+</sup> metal ions showed changes in the spectra, indicating that the three peptoids can coordinate to these metal ions (see the ESI†).

The UV-Vis titration suggested the formation of dinuclear [Fe<sub>2</sub>(**3a–c**)] species. As the titration was carried out with FeCl<sub>3</sub>, we assumed that the counterion, in this case Cl<sup>–</sup>, might help in the coordination of Fe<sup>3+</sup> by bridging.<sup>31</sup> Thus, to gain further insight and to explore the effect of the counterion on Fe<sup>3+</sup> binding, peptoid **3a** was titrated with Fe(ClO<sub>4</sub>)<sub>3</sub> and Fe(NO<sub>3</sub>)<sub>3</sub> under the same reaction conditions as with FeCl<sub>3</sub>. The titration exhibited similar UV-Vis bands to those obtained in the presence of FeCl<sub>3</sub>, including the LMCT band at 570 nm (Fig. 5). The metal-to-peptoid ratio plots also showed a 2 : 1 Fe<sup>3+</sup> to peptoid ratio (see the ESI†). It was therefore concluded that Fe<sup>3+</sup> complexation was independent from the counterion.

ESI-MS spectroscopy (negative mode), performed on the samples of **3a–c** with 2 equiv. of FeCl<sub>3</sub>, further supported the 1 : 2 host : guest ratio evidencing a cluster of pseudomolecular ion peaks with a variable number of solvent molecules bound to the dinuclear complexes (Fig. S16–S18, ESI†). The survey of prominent metalated mass peaks, in conjunction with the experimental isotopic analysis (Fig. S19–S24, ESI†), suggested a general molecular formula, [Fe<sub>2</sub>(**3a–c**)(H<sub>2</sub>O)<sub>*n*</sub>(CH<sub>3</sub>OH)<sub>6–*n*</sub>], confirming the formation of dinuclear complexes rather than a mononuclear one (typical of enterobactin/corynebactin side-

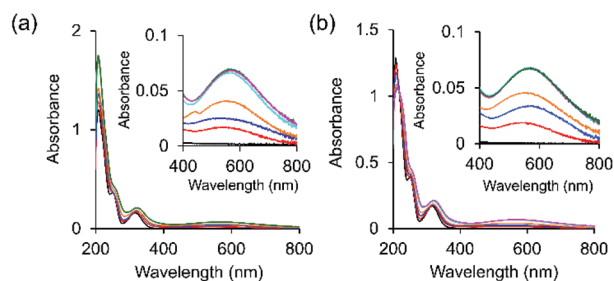


**Fig. 5** UV-Vis titration of **3a** with (a) Fe(ClO<sub>4</sub>)<sub>3</sub> and (b) Fe(NO<sub>3</sub>)<sub>3</sub> in methanol. Peptoid concentration: 17 μM, with additions of 2 μL aliquots of 5 mM methanol solution of Fe<sup>3+</sup> in multiple steps.

rophores).<sup>1</sup> To explore the influence of the solvent on the coordination of Fe<sup>3+</sup>, **3a** was titrated with several aliquots of the Fe<sup>3+</sup> ion in acetonitrile (Fig. S14b†). Saturation was achieved after the addition of 2 equivalents of Fe<sup>3+</sup>, suggesting that the final metallopeptoid complex has a metal:peptoid ratio of 2:1, as observed in methanol. The UV-Vis spectrum in acetonitrile, however, is different from the one obtained in methanol, having two intense maxima near 305 and 372 nm and an LMCT band near 540 nm (Fig. S14c†). Similar solvent dependency of the LMCT band is also reported in the literature for an Fe<sup>3+</sup> phenolate type complex where the LMCT band is observed at a higher wavelength for methanol and is shifted to a lower wavelength in acetonitrile.<sup>32</sup> The solution obtained from the UV-Vis titration was directly analyzed by ESI-MS, which suggests multiple complexes in solution, similar to the spectrum obtained for the titration in methanol; all have a 2:1 metal:peptoid ratio with various solvent molecules as ligands including acetonitrile (see the Experimental section and Fig. S16†). Based on these results we propose that a 2:1 Fe<sup>3+</sup>:peptoid coordination complex is obtained both in methanol and in acetonitrile.

To estimate the affinity of **3a–c** for Fe<sup>3+</sup>, we measured the dissociation constants,  $K_d$ , of the complexes  $[\text{Fe}_2(\mathbf{3a-c})(\text{H}_2\text{O})_n(\text{CH}_3\text{OH})_{6-n}]$  via competition experiments with EDTA.<sup>33,34</sup> As  $K_1 \gg K_2$ , the actual chelator competing with EDTA over Fe<sup>3+</sup> ions was supposed to be BS1, rather than the entire peptoid, and it was reasonable to assume that  $K_d \approx K_1$ .

In a typical experiment a mixture of peptoid and EDTA (16.61  $\mu\text{M}$  of each chelator in methanol) was titrated with Fe<sup>3+</sup>. The UV-Vis signal of these titrations, in the range of 400–800 nm, was monitored according to the method developed by Wedd, and Xiao *et al.*<sup>33</sup> Based on this method, the slope between  $([\text{BS1 site}]_{\text{total}}/[\text{FeBS1}]) - 1$  and  $([\text{EDTA}]_{\text{total}}/[\text{Fe-EDTA}]) - 1$  represented the dissociation constant  $K_d$ . The values obtained were  $K_d = 6.86 \times 10^{-19}$  M,  $4.21 \times 10^{-19}$  M and  $4.01 \times 10^{-19}$  M for  $[\text{Fe}_2(\mathbf{3a-c})(\text{H}_2\text{O})_n(\text{CH}_3\text{OH})_{6-n}]$ , respectively (Fig. S15†). The recorded dissociation constants were higher than those of enterobactin and commercially available siderophores (the log  $K_f$  value for enterobactin, amonabactin T and desferrioxamine E is 49.0, 34.5 and 32.5 respectively).<sup>1</sup>

#### DFT studies on dinuclear $[\text{Fe}_2(\mathbf{3a})(\text{H}_2\text{O})_5(\text{CH}_3\text{OH})]$ complexes

The coordination geometry of the dinuclear complex  $[\text{Fe}_2(\mathbf{3a})(\text{H}_2\text{O})_5(\text{CH}_3\text{OH})]$  emerging from the spectrophotometric and spectrometric studies was investigated by DFT calculations (considering octahedral Fe<sup>3+</sup> ions). Two molecules of water completed the geometry of bis(catecholate)Fe<sup>3+</sup> (BS1); three molecules of water and one of methanol were located on less sterically demanding mono(catecholate)Fe<sup>3+</sup> (BS2).

Dinuclear complex optimization led to pentacoordinated iron centres, as shown by the minimum energy structure reported in Fig. 6. More in detail, one of the water molecules expected to be coordinated to bis(catecholate)Fe<sup>3+</sup>, was, instead, located far away from the metal centre and stabilized by four hydrogen bonds. As for pentacoordinated mono(cate-

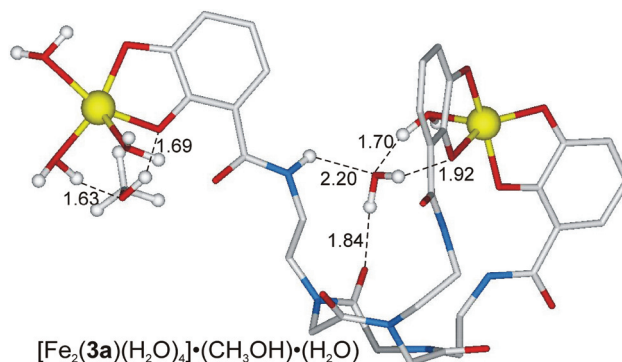


**Fig. 6** Minimum energy structure of  $[\text{Fe}_2(\mathbf{3a})(\text{H}_2\text{O})_4] \cdot (\text{CH}_3\text{OH}) \cdot (\text{H}_2\text{O})$ . Hydrogen atoms are omitted for clarity, except for water and methanol molecules, and for hydrogens involved in hydrogen bonds. Relevant hydrogen bonds are indicated by dashed lines. Distances are given in Å. Atom type: C light grey, N blue, O red, and Fe yellow.

cholate)Fe<sup>3+</sup>, we observed the expulsion of the methanol molecule from the first coordination sphere during the optimization. The final structure  $[\text{Fe}_2(\mathbf{3a})(\text{H}_2\text{O})_4] \cdot (\text{CH}_3\text{OH}) \cdot (\text{H}_2\text{O})$  showed CH<sub>3</sub>OH bound only by hydrogen bonds to the main structure.

Dinuclear complex formation indicated the intrinsic difficulty of the three catecholamide groups to form mononuclear octahedral  $\Lambda$ - $[\text{Fe}(\mathbf{3a})]^{3-}$  species. Our calculations support the formation of a bis(catecholate)Fe<sup>3+</sup> chelating complex (rather than a tris(catecholate)Fe<sup>3+</sup> complex) as suggested by our experimental data. Distorted square pyramidal geometry pentacoordination in BS1 precludes the stereochemical complications discussed for mononuclear complex  $\Lambda$ - $[\text{Fe}(\mathbf{3a})]^{3-}$  and increases the bite angle between the two catecholamide units in  $[\text{Fe}_2(\mathbf{3a})(\text{H}_2\text{O})_4] \cdot (\text{CH}_3\text{OH}) \cdot (\text{H}_2\text{O})$  (from  $\approx 130^\circ$  in  $\Lambda$ - $[\text{Fe}(\mathbf{3a})]^{3-}$  to  $\approx 150^\circ$  in dinuclear complexes).

## Conclusions

New ligands **3a–c** containing three catechol side chains attached to a preorganized cyclotrimeric peptoid scaffold through C<sub>2</sub>, C<sub>4</sub>, and C<sub>6</sub> aliphatic spacers were prepared and spectroscopically characterized. The complexation behaviour of these ligands towards Fe<sup>3+</sup> was first studied at a theoretical level (considering the implications of conformational isomerism of the cyclic peptoid core in conjunction with the octahedral coordination geometry) and then determined through UV-Vis spectrophotometry. The results showed that siderophores **3a–c** display a unique coordination mode forming square pyramidal dinuclear complexes instead of the expected octahedral mononuclear ones, as evident from the UV-Vis titration and MS data. Such exceptional double chelation of Fe<sup>3+</sup>, corroborated by detailed DFT calculations, emphasizes the importance of the backbone structure in the design of novel peptoid-based siderophores.

We are now preparing twelve-membered macrocyclic tricatechol ligands which may more closely mimic the morphologic attributes of enterobactin/corynebactin-type natural ligands and unfold new avenues for the design of novel biostable/bio-compatible ferric ion chelators.

## Experimental

### General procedures

Starting materials and reagents purchased from commercial suppliers were generally used without purification unless otherwise mentioned. TLC was performed on Macherey-Nagel precoated silica gel plates (0.25 mm) and observed under a UV-Vis lamp at 254 nm or sprayed with ninhydrin. HPLC analyses were performed using a JASCO LC-NET II/ADC equipped with a JASCO Model PU-2089 Plus Pump and a JASCO MD-2010 Plus UV-Vis multiple wavelength detector set at 220 nm. The column used was a C<sub>18</sub> reversed-phase analytical column (Waters, Bondapak, 10 μm, 125 Å, 3.9 mm × 300 mm) which runs with linear gradients of ACN (0.1% TFA) in H<sub>2</sub>O (0.1% TFA) over 30 min, at a flow rate of 1.0 mL min<sup>-1</sup>. ESI-MS analysis in the positive ion mode was performed using a Finnigan LCQ Deca ion trap mass spectrometer (ThermoFinnigan, San José, CA, USA) and the mass spectra were acquired and processed using the Xcalibur software provided by Thermo Finnigan. The samples were dissolved in 1:1 CH<sub>3</sub>OH/H<sub>2</sub>O, 0.1% formic acid, and infused in the ESI source by using a syringe pump; the flow rate was 5 μL min<sup>-1</sup>. The capillary voltage was set at 4.0 V, the spray voltage at 5 kV, and the tube lens offset at -40 V. The capillary temperature was 220 °C. Data were acquired in MS1 and MSn scanning modes. Zoom scan was used in these experiments. High-resolution mass spectra (HRMS) were recorded on a Bruker Solarix XR Fourier transform ion cyclotron resonance mass spectrometer (FTICR-MS) equipped with a 7 T magnet, using matrix assisted laser desorption ionization (MALDI) or ESI.† Yields refer to chromatographically and spectroscopically (<sup>1</sup>H- and <sup>13</sup>C NMR) pure materials. NMR spectra were recorded on a Bruker DRX 600 (<sup>1</sup>H at 600.13 MHz, <sup>13</sup>C at 150.90 MHz), and Bruker DRX 400 (<sup>1</sup>H at 400.13 MHz, <sup>13</sup>C at 100.03 MHz). Chemical shifts (δ) are reported in ppm relative to the residual solvent peak (CHCl<sub>3</sub>, δ = 7.26; <sup>13</sup>CDCl<sub>3</sub>, δ = 77.00; C<sub>2</sub>DHCl<sub>4</sub>, CD<sub>2</sub>HOD, δ = 3.31; <sup>13</sup>CD<sub>3</sub>OD, δ = 49.00) and the multiplicity of each signal is designated with the following abbreviations: s, singlet; d, doublet; dd, double doublet; t, triplet; sept, septet; m, multiplet; br, broad. Coupling constants (*J*) are reported in Hertz. For the titration of peptoids with metal ions, UV-Vis measurements were executed using an Agilent Cary 60 UV-Vis spectrophotometer comprising a double beam, Czerny–Turner monochromator. Peptoids **3a–c** titrated with the Fe<sup>3+</sup> ion were directly used for ESI-MS (–ve mode) analysis using an Advion expression CMS mass spectrometer under electrospray ionization (ESI), with direct probe ACN:H<sub>2</sub>O (95:5) at a flow rate of 0.2 mL min<sup>-1</sup>. For isotopic mass analysis, a Bruker Maxis

impact instrument with a direct probe of ACN:H<sub>2</sub>O (70:30) having a flow rate of 0.3 mL min<sup>-1</sup> was used.

### General methods for the preparation of the amines **8a**,<sup>18</sup> **8b**,<sup>19</sup> and **8c**

**Synthesis of derivatives 6a–c.** A catalytic amount of dry dimethylformamide was added, followed by oxalyl chloride (1.50 eq., 1.52 mL, 18.0 mmol) to a dry dichloromethane (48.0 mL) solution of 2,3-bis(benzyloxy)benzoic acid<sup>20</sup> (4.00 g, 12.0 mmol), under a nitrogen atmosphere. The mixture was stirred for 1 hour under a nitrogen atmosphere, then the solvent was evaporated. Dry triethylamine (1.70 eq., 2.84 mL, 0.0200 mmol) was added to the desired *N*-Boc-diamine<sup>21</sup> (11.0 mmol), dissolved in 46.0 mL of dry dichloromethane. The crude residue 2,3-bis(benzyloxy)benzoyl chloride was dissolved in a further 46.0 mL of dry dichloromethane and added dropwise to the reaction mixture. The mixture was stirred at room temperature overnight. CH<sub>2</sub>Cl<sub>2</sub> was removed *in vacuo* to yield a light yellow solid residue. The crude products were purified using flash silica gel, conditions: 100%–95% A (A: dichloromethane; B: methanol), to give known **6a**,<sup>18</sup> and **6b**,<sup>19</sup> and new **6c**.

*N*-(*N*-Boc-ethylenediamine)-2,3-bis(benzyloxy)benzamide (**6a**), light yellow amorphous solid, 3.77 g, 72%. ES-MS: *m/z*; 477.3 [M + H]<sup>+</sup>. <sup>1</sup>H NMR (400 MHz, CDCl<sub>3</sub>) δ: 7.98 (1H, br s, NH), 7.62 (1H, d, *J* 2.4 Hz, *o*-Ar-*H*), 7.38–7.17 (11H, br signals, overlapping, *m*-Ar-*H* and CH<sub>2</sub>-Ph-*H*), 7.06 (1H, d, *J* 1.8 Hz, *p*-Ar-*H*), 5.07 (2H, s, CH<sub>2</sub>-Ph), 5.01 (2H, s, CH<sub>2</sub>-Ph), 3.27 (2H, m, C=O-NH-CH<sub>2</sub>), 3.08 (2H, m, C=OO<sup>t</sup>Bu-NH-CH<sub>2</sub>), 1.32 (9H, s, C=OO(CH<sub>3</sub>)<sub>3</sub>).

*N*-(*N*-Boc-butanediamine)-2,3-bis(benzyloxy)benzamide (**6b**), light yellow amorphous solid, 5.10 g, 92%. ES-MS: *m/z*; 505.2 [M + H]<sup>+</sup>. <sup>1</sup>H NMR (400 MHz, CDCl<sub>3</sub>) δ: 7.93 (1H, br s, NH), 7.74 (1H, br dd, *J* 5.1, 3.7 Hz, *o*-Ar-*H*), 7.48–7.29 (11H, br signals, overlapping, *m*-Ar-*H* and CH<sub>2</sub>-Ph-*H*), 7.15 (1H, br dd, *J* 4.2 Hz, *p*-Ar-*H*), 5.16 (2H, s, CH<sub>2</sub>-Ph), 5.09 (2H, s, CH<sub>2</sub>-Ph), 3.27 (2H, m, C=O-NH-CH<sub>2</sub>), 3.03 (2H, m, C=OO<sup>t</sup>Bu-NH-CH<sub>2</sub>), 1.58 (4H, br signals, overlapping, NH-CH<sub>2</sub>-CH<sub>2</sub>-CH<sub>2</sub>), 1.44 (9H, s, C=OO(CH<sub>3</sub>)<sub>3</sub>).

*N*-(*N*-Boc-hexamethylenediamine)-2,3-bis(benzyloxy)benzamide (**6c**), light yellow amorphous solid, 5.86 g, 100%. ES-MS: *m/z*; 533.6 [M + H]<sup>+</sup>. HRMS (ESI-FTICR) *m/z*; [M + H]<sup>+</sup> calcd for C<sub>32</sub>H<sub>41</sub>N<sub>2</sub>O<sub>5</sub><sup>+</sup> 533.3010; found 533.3031. <sup>1</sup>H NMR (600 MHz, CDCl<sub>3</sub>) δ: 7.90 (1H, m, NH), 7.74 (1H, br dd, *J* 6.2, 3.4 Hz, *o*-Ar-*H*), 7.40–7.30 (11H, br signals, overlapping, *m*-Ar-*H* and CH<sub>2</sub>-Ph-*H*), 7.15 (1H, br dd, *p*-Ar-*H*), 5.16 (2H, s, CH<sub>2</sub>-Ph), 5.08 (2H, s, CH<sub>2</sub>-Ph), 3.25 (2H, m, C=O-NH-CH<sub>2</sub>), 3.07 (2H, m, C=OO<sup>t</sup>Bu-NH-CH<sub>2</sub>), 1.44 (9H, s, C=OO(CH<sub>3</sub>)<sub>3</sub>), 1.42–1.22 (8H, br signals, overlapping, NH-CH<sub>2</sub>-CH<sub>2</sub>-CH<sub>2</sub>-CH<sub>2</sub>-CH<sub>2</sub>-CH<sub>2</sub>).

**Synthesis of derivatives 7a–c.** A solution of trifluoroacetic acid in dry dichloromethane (20% v/v, 77.0 mL) was added dropwise to a dry dichloromethane (77.0 mL) solution of the *N*-Boc protected *N'*-2,3-bis(benzyloxy)benzamides (**6a–c**, 0.0100 mmol), brought to 0 °C in an ice bath. The reaction mixture was stirred at room temperature for 3 hours, then the completion of the reaction was assessed *via* TLC. The solution

was then concentrated *in vacuo* and the crude oil was dissolved in 5.00 mL of hot ethanol, and then added dropwise to 200 mL of a cold 50/50 solution of diethyl ether/petroleum ether to induce the precipitation of known **7a**,<sup>18</sup> and **7b**,<sup>19</sup> and a new **7c** trifluoroacetate salt.

*N*-(Aminoethyl)-2,3-bis(benzyloxy)benzamide, TFA salt (**7a**), white amorphous solid, 3.33 g, 68%. ES-MS: *m/z*; 377.3 [M + H]<sup>+</sup>. <sup>1</sup>H NMR (400 MHz, CDCl<sub>3</sub>) δ: 8.48 (1H, br s, NH), 7.61 (1H, d, *J* 7.5 Hz, *o*-Ar-*H*), 7.41–7.13 (12H, br signals, overlapping, *m*-Ar-*H*, *p*-Ar-*H* and CH<sub>2</sub>-Ph-*H*), 5.17 (2H, s, CH<sub>2</sub>-Ph), 5.13 (2H, s, CH<sub>2</sub>-Ph), 3.33 (2H, m, C=O-NH-CH<sub>2</sub>), 2.96 (2H, m, CH<sub>2</sub>-CH<sub>2</sub>-NH<sub>3</sub><sup>+</sup>).

*N*-(Aminobutyl)-2,3-bis(benzyloxy)benzamide, TFA salt (**7b**), white amorphous solid, 3.63 g, 70%. ES-MS: *m/z*; 405.0 [M + H]<sup>+</sup>. <sup>1</sup>H NMR (400 MHz, CDCl<sub>3</sub>) δ: 8.16 (3H, br s, <sup>+</sup>NH<sub>3</sub>), 8.10 (1H, br s, NH), 7.58 (1H, d, *J* 6.8 Hz, *o*-Ar-*H*), 7.46–7.12 (12H, br signals, overlapping, *m*-Ar-*H*, *p*-Ar-*H* and CH<sub>2</sub>-Ph-*H*), 5.13 (2H, s, CH<sub>2</sub>-Ph), 5.08 (2H, s, CH<sub>2</sub>-Ph), 3.17 (2H, m, C=O-NH-CH<sub>2</sub>), 1.59 (2H, m, CH<sub>2</sub>-CH<sub>2</sub>-NH<sub>3</sub><sup>+</sup>), 1.36 (4H, m, C=O-NH-CH<sub>2</sub>-CH<sub>2</sub>-CH<sub>2</sub>).

*N*-(*N*-Boc-hexamethylenediamine)-2,3-bis(benzyloxy)benzamide, TFA salt (**7c**), white amorphous solid, 2.84 g, 52%. ES-MS: *m/z*; 433.4 [M + H]<sup>+</sup>. HRMS (ESI-FTICR) *m/z*; [M + H]<sup>+</sup> calcd for C<sub>27</sub>H<sub>33</sub>N<sub>2</sub>O<sub>3</sub><sup>+</sup> 433.2486; found 433.2458. <sup>1</sup>H NMR (400 MHz, CDCl<sub>3</sub>) δ: 8.04 (3H, br s, <sup>+</sup>NH<sub>3</sub>), 7.99 (1H, m, NH), 7.57 (1H, dd, *J* 6.2, 3.1 Hz, *o*-Ar-*H*), 7.40–7.07 (11H, br signals, overlapping, *m*-Ar-*H* and CH<sub>2</sub>-Ph-*H*), 7.07 (1H, br dd, *p*-Ar-*H*), 5.08 (2H, s, CH<sub>2</sub>-Ph), 5.01 (2H, s, CH<sub>2</sub>-Ph), 3.12 (2H, q, C=O-NH-CH<sub>2</sub>), 2.85 (2H, m, CH<sub>2</sub>-NH<sub>3</sub><sup>+</sup>), 1.55 (2H, m, CH<sub>2</sub>-CH<sub>2</sub>-NH<sub>3</sub><sup>+</sup>), 1.29–1.10 (6H, overlapping m, NH-CH<sub>2</sub>-CH<sub>2</sub>-CH<sub>2</sub>-CH<sub>2</sub>-CH<sub>2</sub>).

**Synthesis of the free amines** *N*-(aminoethyl)-2,3-bis(benzyloxy)benzamide (**8a**), *N*-(aminobutyl)-2,3-bis(benzyloxy)benzamide (**8b**), and *N*-(aminoethyl)-2,3-bis(benzyloxy)benzamide (**8c**). The TFA salt derivatives (**7a–c**, 0.00600 mmol) were stirred for 30 minutes at room temperature with 25 mL of NaOH 1.25 M. The mixture was extracted three times with 50.0 mL of dichloromethane, then dried over anhydrous MgSO<sub>4</sub> and concentrated *in vacuo* to give known **8a**,<sup>18</sup> and **8b**,<sup>19</sup> and new **8c** as free amines.

*N*-(2-Aminoethyl)-2,3-bis(benzyloxy)benzamide (**8a**), light yellow oil, 2.10 g, 93%. ES-MS: *m/z*; 377.2 [M + H]<sup>+</sup>. <sup>1</sup>H NMR (400 MHz, CDCl<sub>3</sub>) δ: 8.10 (1H, br s, NH), 7.71 (1H, t, *J* 4.7 Hz, *o*-Ar-*H*), 7.46–7.44 (11H, br signals, overlapping, *m*-Ar-*H* and CH<sub>2</sub>-Ph-*H*), 7.12 (1H, d, *J* 4.7 Hz, *p*-Ar-*H*), 5.12 (2H, s, CH<sub>2</sub>-Ph), 5.08 (2H, s, CH<sub>2</sub>-Ph), 3.30 (2H, m, C=O-NH-CH<sub>2</sub>), 2.65 (2H, t, *J* 6.1 Hz, CH<sub>2</sub>-CH<sub>2</sub>-NH<sub>2</sub>), 0.85 (2H, br s, NH<sub>2</sub>).

*N*-(Aminobutyl)-2,3-bis(benzyloxy)benzamide (**8b**), light yellow oil, 2.40 g, 99%. ES-MS: *m/z*; 405.1 [M + H]<sup>+</sup>. <sup>1</sup>H NMR (400 MHz, CDCl<sub>3</sub>) δ: 7.96 (1H, br s, NH), 7.74 (1H, dd, *J* 5.8, 3.7 Hz, *o*-Ar-*H*), 7.48–7.35 (11H, br signals, overlapping, *m*-Ar-*H* and CH<sub>2</sub>-Ph-*H*), 7.15 (1H, d, *J* 3.7 Hz, *p*-Ar-*H*), 5.16 (2H, s, CH<sub>2</sub>-Ph), 5.08 (2H, s, CH<sub>2</sub>-Ph), 3.28 (2H, m, C=O-NH-CH<sub>2</sub>), 2.60 (2H, t, *J* 6.3 Hz, CH<sub>2</sub>-CH<sub>2</sub>-NH<sub>2</sub>), 1.35 (4H, m, C=O-NH-CH<sub>2</sub>-CH<sub>2</sub>-CH<sub>2</sub>).

*N*-(Aminoethyl)-2,3-bis(benzyloxy)benzamide (**8c**), light yellow oil, 2.54 g, 100%. ES-MS: *m/z*; 433.6 [M + H]<sup>+</sup>. HRMS

(ESI-FTICR) *m/z*; [M + H]<sup>+</sup> calcd for C<sub>27</sub>H<sub>33</sub>N<sub>2</sub>O<sub>3</sub><sup>+</sup> 433.2486; found 433.2502. <sup>1</sup>H NMR (400 MHz, CDCl<sub>3</sub>) δ: 7.87 (1H, bt, *J* 6.3 Hz, NH), 7.66 (1H, dd, *J* 6.0, 3.6 Hz, *o*-Ar-*H*), 7.40–7.28 (11H, overlapping, *m*-Ar-*H* and CH<sub>2</sub>-Ph-*H*), 7.07 (1H, m, *p*-Ar-*H*), 5.08 (2H, s, CH<sub>2</sub>-Ph), 4.99 (2H, s, CH<sub>2</sub>-Ph), 3.20 (2H, q, *J* 6.3 Hz, C=O-NH-CH<sub>2</sub>), 2.55 (2H, t, *J* 6.3 Hz, CH<sub>2</sub>-NH<sub>2</sub>), 1.26 (4H, m, CH<sub>2</sub>-CH<sub>2</sub>-NH<sub>2</sub> and NH-CH<sub>2</sub>-CH<sub>2</sub>), 1.15 (4H, overlapping m, NH-CH<sub>2</sub>-CH<sub>2</sub>-CH<sub>2</sub>-CH<sub>2</sub>). <sup>13</sup>C NMR (100 MHz, CDCl<sub>3</sub>) δ: 164.9 (C=O), 151.5 (*m*-C-OBn), 146.5 (*o*-C-OBn), 136.2 × 2 (C-Ph), 128.6 × 3 (C-Ph), 128.5 × 3 (C-Ph), 128.1 × 2 (C-Ph), 127.5 × 3 (C-Ph), 124.3 (*p*-C-Ar), 123.0 (*o*-C-Ar), 116.6 (*m*-C-Ar), 76.2 (O-CH<sub>2</sub>-Ph), 71.0 (O-CH<sub>2</sub>-Ph), 41.3 (CH<sub>2</sub>-NH<sub>2</sub>), 39.4 (C=O-NH-CH<sub>2</sub>), 32.2 (CH<sub>2</sub>-CH<sub>2</sub>-NH<sub>2</sub>), 29.0 (C=O-NH-CH<sub>2</sub>-CH<sub>2</sub>), 26.5 (C=O-NH-CH<sub>2</sub>-CH<sub>2</sub>-CH<sub>2</sub>), 26.2 (CH<sub>2</sub>-CH<sub>2</sub>-CH<sub>2</sub>-NH<sub>2</sub>).

## General methods for the synthesis of the peptoid derivatives

**Solid-phase synthesis of the linear precursors 9a–c.** The 2-chlorotrityl chloride resin ( $\alpha$ -dichlorobenzhydryl-polystyrene cross-linked with 1% DVB; 100–200 mesh; 1.47 mmol g<sup>-1</sup>, 0.300 g, 0.441 mmol) was swelled in dry CH<sub>2</sub>Cl<sub>2</sub> (3 mL) for 45 min and washed twice with CH<sub>2</sub>Cl<sub>2</sub> (3 mL). The first submonomer was attached to the resin by adding bromoacetic acid (0.0980 g, 0.706 mmol) in dry CH<sub>2</sub>Cl<sub>2</sub> (3 mL) and DIPEA (384  $\mu$ L, 2.20 mmol) on a shaker platform for 60 min at room temperature, followed by washing with DMF (3 × 1 min), CH<sub>2</sub>Cl<sub>2</sub> (3 × 1 min) and again with DMF (3 × 1 min). A solution of the chosen amine (2.20 mmol, 1.63 M in dry DMF) was added to the bromoacetylated resin. The mixture was left on a shaker platform for 60 min at room temperature, then the resin was washed with DMF (3 × 1 min), CH<sub>2</sub>Cl<sub>2</sub> (3 × 1 min) and again with DMF (3 × 1 min). Subsequent bromoacetylation reactions were accomplished by reacting the aminated oligomer with a solution of bromoacetic acid (0.613 g, 4.41 mmol) and DIC (751  $\mu$ L, 4.85 mmol) in dry DMF (3 mL) for 60 min at room temperature; the completion of the reaction was assessed with the chloranil test. The filtered resin was washed with DMF (3 × 1 min), CH<sub>2</sub>Cl<sub>2</sub> (3 × 1 min), and again DMF (3 × 1 min) and then treated again with the appropriate amine under the same conditions reported above. This cycle of reactions was iterated until the target linear trimer was obtained. The cleavage process was performed by treating the resin, previously washed with CH<sub>2</sub>Cl<sub>2</sub> (6 × 1 min), three times with a solution of HFIP in CH<sub>2</sub>Cl<sub>2</sub> (20% v/v, 3.00 mL each time) on a shaker platform at room temperature for 30 min each time. The resin was then filtered away and the combined filtrates were concentrated *in vacuo*. 1 mg of the final products was dissolved in 60  $\mu$ L of acetonitrile (0.1% TFA) and 60  $\mu$ L of HPLC grade water (0.1% TFA) and analyzed by RP-HPLC; purity >80%; conditions: 5 → 100% A in 30 min (A, 0.1% TFA in acetonitrile, B, 0.1% TFA in water); flow: 1.0 mL min<sup>-1</sup>, 220 nm. The linear oligomers (isolated as amorphous solids) were subjected to HRMS and, subsequently, to the cyclization reactions without further purification.

(9a): white amorphous solid, 0.558 g, 100%;  $t_R$ : 15.0 min. ES-MS  $m/z$ ; HRMS (MALDI-FTICR)  $m/z$ ;  $[M + H]^+$  calcd for  $C_{75}H_{75}N_6O_{13}^+$  1267.5387; found 1267.5375.

(9b): white amorphous solid, 0.578 g, 97%;  $t_R$ : 20.0 min. ES-MS  $m/z$ ; HRMS (MALDI-FTICR)  $m/z$ ;  $[M + H]^+$  calcd for  $C_{81}H_{87}N_6O_{13}^+$  1351.6326; found 1351.6390.

(9c): white amorphous solid, 0.531 g, 84%;  $t_R$ : 19.3 min. ES-MS  $m/z$ ; HRMS (MALDI-FTICR)  $m/z$ ;  $[M + H]^+$  calcd for  $C_{87}H_{99}N_6O_{13}^+$  1435.7265; found 1435.7241.

**Cyclization procedure: synthesis of the cyclic peptoids 10a–c.** The solutions of the linear peptoids (0.300 mmol), previously co-evaporated three times with toluene, were prepared under nitrogen in dry DMF (15.0 mL). The mixture was added dropwise to a stirred solution of HATU (0.456 g, 1.20 mmol) and DIPEA (324  $\mu$ L, 1.86 mmol) in dry DMF (85.0 mL) by using a syringe pump in 6 h, at room temperature in an anhydrous atmosphere. After 12 h the resulting mixture was concentrated *in vacuo*, diluted with  $CH_2Cl_2$  (60.0 mL), and washed twice with a solution of HCl (1.00 M, 30.0 mL). The organic phase was washed with water (60.0 mL), dried over anhydrous  $MgSO_4$ , filtered and concentrated *in vacuo*. The crude cyclic peptoids were purified using flash silica gel; conditions: 1 : 1 petroleum ether : ethyl acetate, then 100% ethyl acetate, and, finally, 90 : 10 ethyl acetate : methanol. The cyclic peptoids were dissolved in 50% acetonitrile in HPLC grade water and analysed by RP-HPLC; purity >90% conditions: 5%–100% A in 30 min (A, 0.1% TFA in acetonitrile, B, 0.1% TFA in water); flow: 1 mL  $min^{-1}$ , 220 nm, subsequently characterized *via*  $^1H$ - and  $^{13}C$ -NMR spectroscopy and HRMS (MALDI-FTICR).

(10a): white amorphous solid, 0.0900 g, 24%;  $t_R$ : 20.2 min. HRMS (MALDI-FTICR)  $m/z$ ;  $[M + H]^+$  calcd for  $C_{75}H_{73}N_6O_{12}^+$  1249.5281; found 1249.5296;  $[M + Na]^+$  calcd for  $C_{75}H_{72}N_6NaO_{12}^+$  1271.5100; found 1249.5113.  $^1H$  NMR (600 MHz,  $CDCl_3$ )  $\delta$ : 7.85 (3H, br t, NH), 7.60 (3H, dd,  $J$  6.5, 2.9 Hz, *o*-Ar-*H*), 7.46–7.45 (6H, overlapping, *o*- $CH_2$ -Ph-*H*), 7.40–7.30 (21H, overlapping, *m*-Ar-*H* and *m*- $CH_2$ -Ph-*H*), 7.11–7.10 (9H, overlapping signals, *p*-Ar-*H* and *p*- $CH_2$ -Ph-*H*), 5.13 (6H, s,  $CH_2$ -Ph), 5.07 (6H, s,  $CH_2$ -Ph), 4.17 (3H, d,  $J$  15.6 Hz, C=O-*CHH*-N), 3.88 (3H, m, C=O-NH-*CHH*), 3.62 (3H, m, C=O-NH-*CHH*), 3.47 (3H, d,  $J$  15.6 Hz, C=O-*CHH*-N), 3.27–3.23 (6H, overlapping m, N- $CH_2$ - $CH_2$ -NH).  $^{13}C$  NMR (150 MHz,  $CDCl_3$ )  $\delta$ : 167.7  $\times$ 3 (C=O-N), 165.8  $\times$ 3 (C=O-NH), 151.8  $\times$ 3 (*m*-C-OBn), 146.7  $\times$ 3 (*o*-C-OBn), 136.6  $\times$ 3 (O- $CH_2$ -C), 136.4  $\times$ 3 (O- $CH_2$ -C), 128.9  $\times$ 3 (C-Ph), 128.6  $\times$ 12 (C-Ph), 128.2  $\times$ 3 (C-Ph), 127.6  $\times$ 12 (C-Ph), 124.3  $\times$ 3 (*m*-C-Ar), 122.8  $\times$ 3 (*o*-C-Ar), 116.9  $\times$ 3 (*p*-C-Ar), 76.2  $\times$ 3 (O- $CH_2$ -Ph), 71.2  $\times$ 3 (O- $CH_2$ -Ph), 48.7  $\times$ 3 (C=O- $CH_2$ -N), 46.1  $\times$ 3 (C=O-NH- $CH_2$ ), 36.7  $\times$ 3 (C=O-N- $CH_2$ ).

(10b): white amorphous solid, 0.0960 g, 24%;  $t_R$ : 18.4 min. HRMS (MALDI-FTICR)  $m/z$ ;  $[M + H]^+$  calcd for  $C_{81}H_{85}N_6O_{12}^+$  1333.6220; found 1333.6246.  $^1H$  NMR (600 MHz,  $CDCl_3$ )  $\delta$ : 7.99 (3H, br t, NH), 7.69 (3H, dd,  $J$  7.6, 1.8 Hz, *o*-Ar-*H*), 7.46–7.45 (6H, overlapping, *o*- $CH_2$ -Ph-*H*) 7.40–7.33 (21H, overlapping, *m*-Ar-*H* and *m*- $CH_2$ -Ph-*H*), 7.13–7.08 (9H, overlapping signals, *p*-Ar-*H* and *p*- $CH_2$ -Ph-*H*), 5.14 (6H, s,  $CH_2$ -Ph), 5.08 (6H, s,  $CH_2$ -Ph), 4.63 (3H, d,  $J$  15.5 Hz, C=O-*CHH*-N), 3.76

(3H, m, C=O-NH-*CHH*), 3.54 (3H, d,  $J$  15.5 Hz, C=O-*CHH*-N), 3.27–3.20 (9H, overlapping m, C=O-NH-*CHH* and N- $CH_2$ - $CH_2$ - $CH_2$ -NH), 1.47 (6H, m, N- $CH_2$ - $CH_2$ - $CH_2$ -NH), 1.27 (6H, m, N- $CH_2$ - $CH_2$ - $CH_2$ -NH).  $^{13}C$  NMR (150 MHz,  $CDCl_3$ )  $\delta$ : 167.2  $\times$ 3 (C=O-N), 165.3  $\times$ 3 (C=O-NH), 151.7  $\times$ 3 (*m*-C-OBn), 146.8  $\times$ 3 (*o*-C-OBn), 136.4  $\times$ 6 (O- $CH_2$ -C), 128.7  $\times$ 3 (C-Ph), 128.2  $\times$ 12 (C-Ph), 127.7  $\times$ 3 (C-Ph), 127.2  $\times$ 12 (C-Ph), 124.4  $\times$ 3 (*m*-C-Ar), 123.2  $\times$ 3 (*o*-C-Ar), 117.0  $\times$ 3 (*p*-C-Ar), 76.4  $\times$ 3 (O- $CH_2$ -Ph), 71.3  $\times$ 3 (O- $CH_2$ -Ph), 48.9  $\times$ 3 (C=O- $CH_2$ -N), 46.5  $\times$ 3 (C=O-NH- $CH_2$ ), 38.9  $\times$ 3 (C=O-N- $CH_2$ ), 26.6  $\times$ 3 (N- $CH_2$ - $CH_2$ - $CH_2$ - $CH_2$ -NH), 23.8  $\times$ 3 (N- $CH_2$ - $CH_2$ - $CH_2$ - $CH_2$ -NH).

(10c): white amorphous solid, 0.0510 g, 12%;  $t_R$ : 22.1 min. HRMS (MALDI-FTICR)  $m/z$ ;  $[M + H]^+$  calcd for  $C_{87}H_{97}N_6O_{12}^+$  1417.7159; found 1417.7185.  $^1H$  NMR (600 MHz,  $CDCl_3$ )  $\delta$ : 7.90 (3H, br t, NH), 7.72 (3H, dd,  $J$  5.4, 4.2 Hz, *o*-Ar-*H*), 7.47–7.46 (6H, overlapping, *o*- $CH_2$ -Ph-*H*), 7.41–7.33 (21H, overlapping, *m*-Ar-*H* and *m*- $CH_2$ -Ph-*H*), 7.14–7.13 (9H, overlapping signals, *p*-Ar-*H* and *p*- $CH_2$ -Ph-*H*), 5.15 (6H, s,  $CH_2$ -Ph), 5.07 (6H, s,  $CH_2$ -Ph), 4.66 (3H, d,  $J$  15.3 Hz, C=O-*CHH*-N), 3.80 (3H, m, C=O-NH-*CHH*), 3.56 (3H, d,  $J$  15.3 Hz, C=O-*CHH*-N), 3.26–3.19 (9H, overlapping m, C=O-NH-*CHH* and N- $CH_2$ - $CH_2$ - $(CH_2)_2$ - $CH_2$ - $CH_2$ -NH), 1.47 (6H, m, N- $CH_2$ - $CH_2$ - $(CH_2)_2$ - $CH_2$ - $CH_2$ -NH), 1.33–1.20 (18H, overlapping m, N- $CH_2$ - $CH_2$ - $(CH_2)_2$ - $CH_2$ - $CH_2$ -NH).  $^{13}C$  NMR (150 MHz,  $CDCl_3$ )  $\delta$ : 167.0  $\times$ 3 (C=O-N), 165.0  $\times$ 3 (C=O-NH), 151.7  $\times$ 3 (*m*-C-OBn), 146.8  $\times$ 3 (*o*-C-OBn), 136.5  $\times$ 6 (O- $CH_2$ -C), 128.7  $\times$ 15 (C-Ph), 127.7  $\times$ 3 (C-Ph), 127.2  $\times$ 12 (C-Ph), 124.4  $\times$ 3 (*m*-C-Ar), 123.4  $\times$ 3 (*o*-C-Ar), 117.0  $\times$ 3 (*p*-C-Ar), 76.4  $\times$ 3 (O- $CH_2$ -Ph), 71.4  $\times$ 3 (O- $CH_2$ -Ph), 49.0  $\times$ 3 (C=O- $CH_2$ -N), 47.1  $\times$ 3 (C=O-NH- $CH_2$ ), 39.4  $\times$ 3 (C=O-N- $CH_2$ ), 29.1  $\times$ 3 (N- $CH_2$ - $CH_2$ - $(CH_2)_2$ - $CH_2$ - $CH_2$ -NH), 26.6  $\times$ 3 (N- $CH_2$ - $CH_2$ - $(CH_2)_2$ - $CH_2$ - $CH_2$ -NH), 26.4  $\times$ 3 (N- $CH_2$ - $CH_2$ - $(CH_2)_2$ - $CH_2$ - $CH_2$ -NH), 26.3  $\times$ 3 (N- $CH_2$ - $CH_2$ - $(CH_2)_2$ - $CH_2$ - $CH_2$ -NH).

**Hydrogenation procedure: synthesis of the ligands 3a–c.** To a solution of cyclic peptoids 10a–c (0.0300 mmol), in ethyl acetate (0.430 mL), Pd 10% wt on carbon was added (half of the weight with respect to the cyclic peptoid substrate). Three cycles of *vacuum*-hydrogen were performed, and the reaction was stirred for 5 hours. After 5 hours, 0.860 mL of ethanol was added, and three more *vacuum*-hydrogen cycles were performed. The reaction mixture was stirred for an additional 19 hours, then the completion of the reaction was assessed *via* TLC. The reaction mixture was filtered with ethanol using a Celite pad and extensively dried *in vacuo* to obtain the final products. The cyclic peptoids were dissolved in 50% acetonitrile in HPLC grade water and analysed by RP-HPLC; purity >90% conditions: 5%–100% A in 30 min (A, 0.1% TFA in acetonitrile, B, 0.1% TFA in water); flow: 1 mL  $min^{-1}$ , 220 nm, subsequently characterized *via*  $^1H$ - and  $^{13}C$ -NMR spectroscopy and HRMS (MALDI-FTICR).

(3a): white amorphous solid, 0.0210 g, 100%;  $t_R$ : 9.9 min. HRMS (MALDI-FTICR)  $m/z$ ;  $[M + Na]^+$  calcd for  $C_{33}H_{36}N_6NaO_{12}^+$  731.2283; found 731.2293.  $^1H$  NMR (600 MHz,  $CD_3OD$ )  $\delta$ : 7.12 (3H, dd,  $J$  8.2, 1.1 Hz, *o*-Ar-*H*), 6.90 (3H, dd,  $J$  8.2, 1.1 Hz, *m*-Ar-*H*), 6.68 (3H, t,  $J$  8.1 Hz, *p*-Ar-*H*), 5.13 (3H, d,  $J$  15.8 Hz, C=O-*CHH*-N), 3.86 (3H, m, C=O-NH-

CHH), 3.69 (3H, d,  $J$  15.8 Hz, C=O-CHH-N), 3.61–3.57 (9H, overlapping m, C=O-NH-CHH and N-CH<sub>2</sub>-CH<sub>2</sub>-NH). <sup>13</sup>C NMR (150 MHz, CD<sub>3</sub>OD)  $\delta$ : 171.8  $\times$ 3 (C=O-N), 170.7  $\times$ 3 (C=O-NH), 150.4  $\times$ 3 (*o*-C-OH), 147.3  $\times$ 3 (*m*-C-OH), 119.7  $\times$ 3 (*p*-C-Ar), 119.6  $\times$ 3 (*m*-C-Ar), 118.7  $\times$ 3 (*o*-C-Ar), 116.6  $\times$ 3 (C=O-C-Ar), 51.0  $\times$ 3 (C=O-CH<sub>2</sub>-N), 48.3  $\times$ 3 (C=O-NH-CH<sub>2</sub>), 38.0  $\times$ 3 (C=O-N-CH<sub>2</sub>).

(3b): white amorphous solid, 0.0240 g, 100%;  $t_R$ : 11.5 min. HRMS (MALDI-FTICR)  $m/z$ ; [M + H]<sup>+</sup> calcd for C<sub>39</sub>H<sub>49</sub>N<sub>6</sub>O<sub>12</sub><sup>+</sup> 793.3403; found 793.3389. <sup>1</sup>H NMR (600 MHz, CD<sub>3</sub>OD)  $\delta$ : 7.21 (3H, dd,  $J$  8.1, 1.1 Hz, *o*-Ar-*H*), 6.91 (3H, dd,  $J$  8.1, 1.1 Hz, *m*-Ar-*H*), 6.70 (3H, t,  $J$  8.0 Hz, *p*-Ar-*H*), 5.11 (3H, d,  $J$  15.6 Hz, C=O-CHH-N), 3.65 (3H, m, C=O-NH-CHH), 3.62 (3H, d,  $J$  15.6 Hz, C=O-CHH-N), 3.45–3.35 (9H, overlapping m, C=O-NH-CHH and N-CH<sub>2</sub>-CH<sub>2</sub>-CH<sub>2</sub>-CH<sub>2</sub>-NH), 1.67–1.53 (12H, overlapping m, N-CH<sub>2</sub>-CH<sub>2</sub>-CH<sub>2</sub>-CH<sub>2</sub>-NH). <sup>13</sup>C NMR (150 MHz, CD<sub>3</sub>OD)  $\delta$ : 171.6  $\times$ 3 (C=O-N), 170.1  $\times$ 3 (C=O-NH), 150.3  $\times$ 3 (*o*-C-OH), 147.3  $\times$ 3 (*m*-C-OH), 119.6  $\times$ 6 (*p*-C-Ar and *m*-C-Ar), 118.6  $\times$ 3 (*o*-C-Ar), 116.8  $\times$ 3 (C=O-C-Ar), 50.8  $\times$ 3 (C=O-CH<sub>2</sub>-N), 40.0  $\times$ 3 (C=O-NH-CH<sub>2</sub>), 27.6  $\times$ 3 (C=O-N-CH<sub>2</sub>), 25.1  $\times$ 6 (N-CH<sub>2</sub>-CH<sub>2</sub>-CH<sub>2</sub>-CH<sub>2</sub>-NH).

(3c): white amorphous solid, 0.0260 g, 100%;  $t_R$ : 14.0 min. HRMS (MALDI-FTICR)  $m/z$ ; [M + H]<sup>+</sup> calcd for C<sub>45</sub>H<sub>61</sub>N<sub>6</sub>O<sub>12</sub><sup>+</sup> 877.4342; found 877.4353. <sup>1</sup>H NMR (600 MHz, CD<sub>3</sub>OD)  $\delta$ : 7.21 (3H, d,  $J$  7.8 Hz, *o*-Ar-*H*), 6.92 (3H, d,  $J$  7.8 Hz, *m*-Ar-*H*), 6.70 (3H, t,  $J$  7.8 Hz, *p*-Ar-*H*), 5.08 (3H, d,  $J$  15.6 Hz, C=O-CHH-N), 3.65 (3H, m, C=O-NH-CHH), 3.58 (3H, d,  $J$  15.6 Hz, C=O-CHH-N), 3.40–3.36 (9H, overlapping m, C=O-NH-CHH and N-CH<sub>2</sub>-CH<sub>2</sub>-(CH<sub>2</sub>)<sub>2</sub>-CH<sub>2</sub>-CH<sub>2</sub>-NH), 1.63–1.56 (12H, overlapping m, N-CH<sub>2</sub>-CH<sub>2</sub>-(CH<sub>2</sub>)<sub>2</sub>-CH<sub>2</sub>-CH<sub>2</sub>-NH and N-CH<sub>2</sub>-CH<sub>2</sub>-(CH<sub>2</sub>)<sub>2</sub>-CH<sub>2</sub>-CH<sub>2</sub>-NH), 1.42–1.29 (12H, overlapping m, N-CH<sub>2</sub>-CH<sub>2</sub>-(CH<sub>2</sub>)<sub>2</sub>-CH<sub>2</sub>-CH<sub>2</sub>-NH). <sup>13</sup>C NMR (150 MHz, CD<sub>3</sub>OD)  $\delta$ : 171.4  $\times$ 3 (C=O-N), 170.1  $\times$ 3 (C=O-NH), 150.3  $\times$ 3 (*o*-C-OH), 147.3  $\times$ 3 (*m*-C-OH), 119.6  $\times$ 6 (*p*-C-Ar and *m*-C-Ar), 118.7  $\times$ 3 (*o*-C-Ar), 116.9  $\times$ 3 (C=O-C-Ar), 50.8  $\times$ 3 (C=O-CH<sub>2</sub>-N), 40.3  $\times$ 3 (C=O-NH-CH<sub>2</sub>), 30.2  $\times$ 3 (C=O-N-CH<sub>2</sub>), 27.6  $\times$ 3 (N-CH<sub>2</sub>-CH<sub>2</sub>-(CH<sub>2</sub>)<sub>2</sub>-CH<sub>2</sub>-CH<sub>2</sub>-NH), 27.5  $\times$ 3 (N-CH<sub>2</sub>-CH<sub>2</sub>-(CH<sub>2</sub>)<sub>2</sub>-CH<sub>2</sub>-CH<sub>2</sub>-NH), 27.4  $\times$ 6 (N-CH<sub>2</sub>-CH<sub>2</sub>-(CH<sub>2</sub>)<sub>2</sub>-CH<sub>2</sub>-CH<sub>2</sub>-NH).

### UV-Vis titrations

The titration experiments of peptoids 3a–c with metal ions (Co<sup>2+</sup>, Cu<sup>2+</sup>, Ni<sup>2+</sup>, Zn<sup>2+</sup>, Fe<sup>2+</sup> and Fe<sup>3+</sup>) were carried out in methanol solvent medium. Co<sup>2+</sup>, Cu<sup>2+</sup>, Ni<sup>2+</sup>, Zn<sup>2+</sup>, Fe<sup>3+</sup> were used as chloride salts, and Fe<sup>2+</sup> was used as a perchlorate salt. After recording the blank spectrum of methanol in the 200–800 nm range, 10  $\mu$ L of peptoids 3a–c (5 mM stock solution) was diluted in 3 mL of the solvent (MeOH here) to obtain a concentration of 17  $\mu$ M. The peptoids were further titrated with various metal ions individually with 2  $\mu$ L aliquots each time; the concentration of the metal ion stock solution was 5 mM in methanol. A similar titration was carried out at 8  $\mu$ M concentration of 3a with the addition of several aliquots of Fe<sup>3+</sup> in acetonitrile. In particular, 5  $\mu$ L of peptoid 3a (5 mM stock solution in methanol) was diluted in 3 mL of acetonitrile to obtain a concentration of 8  $\mu$ M and titrated with 0.5 equi-

valent of the Fe<sup>3+</sup> ion each time. For MS analysis of the titrated acetonitrile solution see Fig. S16.†

### Dissociation constant calculations

The dissociation constants for Fe<sup>3+</sup> with peptoids 3a–c were measured by using UV-Vis spectroscopy following a competition method. The stock solutions of peptoids 3a–c, EDTA and Fe<sup>3+</sup> were prepared at 5 mM concentration in methanol. For EDTA, the solvent was water and the pH value was maintained at 7. In a competition experiment,<sup>33,34</sup> peptoids (3a–c individually) and EDTA were taken in a 1 : 1 ratio at 16.61  $\mu$ M and gradually titrated with Fe<sup>3+</sup> up to two equivalents. The UV-Vis spectra were monitored in the 400–800 nm range. Following the method reported by Wedd and Xiao *et al.*, the slope between ([BS1 site]<sub>total</sub>/[FeBS1]) – 1 and ([EDTA]<sub>total</sub>/[Fe-EDTA]) – 1 was calculated. The slope equals to  $K_{d(\text{Fe-Peptoid})}K_{a(\text{Fe-EDTA})}\alpha_{(\text{EDTA})}$  where  $K_{d(\text{Fe-Peptoid})}$  is the dissociation constant of Fe-peptoid,  $K_{a(\text{Fe-EDTA})}$  is the association constant of Fe-EDTA complexation and  $\alpha_{(\text{EDTA})}$  is the pH correction factor for EDTA (see the ESI†).

### Conflicts of interest

There are no conflicts to declare.

### Acknowledgements

PG is thankful to Dr Zhiguang Xiao from The Florey Institute of Neuroscience and Mental Health, Australia for many helpful discussions and suggestions. PG gratefully acknowledges the Lady Davis Fellowship Trust, Technion-Israel Institute of Technology for a postdoctoral fellowship. Financial support from the University of Salerno (FARB) is acknowledged. We thank Dr Patrizia Iannece, University of Salerno, for HR-MS, and Dr Patrizia Oliva, University of Salerno, for NMR spectra.

### Notes and references

- 1 R. C. Hider and X. Kong, *Nat. Prod. Rep.*, 2010, **27**, 637.
- 2 N. Abbaspour, R. Hurrell and R. Kelishadi, *J. Res. Med. Sci.*, 2014, **19**, 164.
- 3 C. Kurth, H. Kageband and M. Nett, *Org. Biomol. Chem.*, 2016, **14**, 8212.
- 4 A. Szebesczyk, E. Olshvang, A. Shanzer, P. L. Carver and E. Gumienna-Kontecka, *Coord. Chem. Rev.*, 2016, **327–328**, 84.
- 5 P. Tyagi, Y. Kumar, D. Gupta, H. Singh and A. Kumar, *Int. J. Pharm. Pharm. Sci.*, 2015, **7**, 35.
- 6 A. Maggio, *Br. J. Haematol.*, 2007, **138**, 407.
- 7 M. H. Urgesa and B. Y. Hirpaye, *J. Chem. Pharm. Res.*, 2017, **9**, 182.
- 8 K. N. Raymond, E. A. Dertz and S. S. Kim, *Proc. Natl. Acad. Sci. U. S. A.*, 2003, **100**, 3584.
- 9 (a) M. E. Bluhm, S. S. Kim, E. A. Dertz and K. N. Raymond, *J. Am. Chem. Soc.*, 2002, **124**, 2436; (b) K. N. Raymond, B. E. Allred and A. K. Sia, *Acc. Chem. Res.*, 2015, **48**, 2496.

- 10 W. H. Rastetter, T. J. Erickson and M. C. Venuti, *J. Org. Chem.*, 1981, **46**, 3579.
- 11 (a) M. M. Andrade and A. P. Rauter, *Carbohydr. Chem.*, 2012, **38**, 398; (b) A. Müller, A. J. Wilkinson, K. S. Wilson and A.-K. Duhme-Klair, *Angew. Chem., Int. Ed.*, 2006, **45**, 5132; (c) T. D. P. Stack, T. B. Karpishin and K. N. Raymond, *J. Am. Chem. Soc.*, 1992, **114**, 1512; (d) M. C. Venuti, W. H. Rastetter and J. B. Neilands, *J. Med. Chem.*, 1979, **22**, 123; (e) S. J. Rodgers, C.-W. Lee, C. Y. Ng and K. N. Raymond, *Inorg. Chem.*, 1987, **26**, 1622; (f) M. Albrecht, *Chem. Soc. Rev.*, 1998, **27**, 281.
- 12 S. M. Miller, R. J. Simon, S. Ng, R. N. Zuckermann, J. M. Kerr and W. H. Moos, *Bioorg. Med. Chem. Lett.*, 1994, **4**, 2657.
- 13 A. D'Amato, R. Schettini, G. Della Sala, C. Costabile, C. Tedesco, I. Izzo and F. De Riccardis, *Org. Biomol. Chem.*, 2017, **15**, 9932.
- 14 C. Wolf, *Dynamic Stereochemistry of Chiral Compounds. Principles and Applications*, RCS Publishing, 2008.
- 15 F. De Riccardis, *Eur. J. Org. Chem.*, 2020, DOI: 10.1002/ejoc.201901838.
- 16 A. D'Amato, G. Pierri, C. Tedesco, G. Della Sala, I. Izzo, C. Costabile and F. De Riccardis, *J. Org. Chem.*, 2019, **84**, 10911.
- 17 R. N. Zuckermann, J. M. Kerr, S. B. H. Kent and W. H. Moos, *J. Am. Chem. Soc.*, 1992, **114**, 10646.
- 18 Q. Zhang, B. Jin, R. Peng, S. Lei and S. Chu, *Polyhedron*, 2015, **87**, 417.
- 19 S. Lei, B. Jin, Q. Zhang, Z. Zhang, X. Wang, R. Peng and S. Chu, *Polyhedron*, 2016, **119**, 387.
- 20 S. Kishimoto, S. Nishimura and H. Kakeya, *Chem. Lett.*, 2015, **44**, 1303.
- 21 S. Jobin, S. Vézina-Dawod, C. Herby, A. Derson and E. Biron, *Org. Lett.*, 2015, **17**, 5626.
- 22 C. Tedesco, L. Erra, I. Izzo and F. De Riccardis, *CrystEngComm*, 2014, **16**, 3667.
- 23 N. Maulucci, I. Izzo, G. Bifulco, A. Aliberti, C. De Cola, D. Comegna, C. Gaeta, A. Napolitano, C. Pizza, C. Tedesco, D. Flot and F. De Riccardis, *Chem. Commun.*, 2008, 3927.
- 24 A. S. Culf, M. Čuperlović-Culf, D. A. Léger and A. Decken, *Org. Lett.*, 2014, **16**, 2780.
- 25 R. J. Kurland, M. B. Rubin and W. B. Wise, *J. Chem. Phys.*, 1964, **40**, 2426.
- 26 G. Maayan, N. Gluz and G. Christou, *Nat. Catal.*, 2018, **1**, 48.
- 27 Q. Zhang, B. Jin, X. Wang, S. Lei, Z. Shi, J. Zhao, Q. Liu and R. Peng, *R. Soc. Open Sci.*, 2018, **5**, 171492.
- 28 S. L. Jewett, S. Egging and L. Geller, *J. Inorg. Biochem.*, 1997, **66**, 165.
- 29 J. P. Nandre, S. R. Patil, S. K. Sahoo, C. P. Pradeep, A. Churakov, F. Yu, L. Chen, C. Redshaw, A. A. Patil and U. D. Patil, *Dalton Trans.*, 2017, **46**, 14201.
- 30 M. T. Stauffer and S. G. Weber, *Anal. Chem.*, 1999, **71**, 1146.
- 31 E. Viñuelas-Zahínos, F. Luna-Giles, P. Torres-García and A. Bernalte-García, *Polyhedron*, 2009, **28**, 1362.
- 32 R. K. Dean, C. I. Fowler, K. Hasan, K. Kerman, P. Kwong, S. Trudel, D. B. Leznoff, H.-B. Kraatz, L. N. Dawe and C. M. Kozak, *Dalton Trans.*, 2012, **41**, 4806.
- 33 L. Zhang, M. Koay, M. J. Maher, Z. Xiao and A. G. Wedd, *J. Am. Chem. Soc.*, 2006, **128**, 5834.
- 34 Z. Xiao and A. G. Wedd, *Nat. Prod. Rep.*, 2010, **27**, 768.